Blue Organic Light-Emitting Diode with a Turn-on Voltage at 1.47 V

Seiichiro Izawa[1,2], Masahiro Morimoto[3*], Keisuke Fujimoto[4*], Koki Banno[4], Yutaka Majima[1], Masaki Takahashi[4], Shigeki Naka[3], and Masahiro Hiramoto[5]*

[1]Laboratory for Materials and Structures, Tokyo Institute of Technology, 4259 Nagatsuta-cho, Midori-ku, Yokohama, Kanagawa 226-8503, Japan. [2]Precursory Research for Embryonic Science and Technology (PRESTO), Japan Science and Technology Agency (JST), 4-1-8 Honcho, Kawaguchi, Saitama 332-0012, Japan. [3]Academic Assembly Faculty of Engineering, University of Toyama, 3190 Gofuku, Toyama 930-8555, Japan. [4]Department of Applied Chemistry, Faculty of Engineering, Shizuoka University, 3-5-1 Johoku, Naka-ku, Hamamatsu, Shizuoka, 432-8561, Japan. [5]Institute for Molecular Science, 5-1 Higashiyama, Myodaiji, Okazaki 444-8787, Aichi, Japan

E-Mail: izawa.s.ac@m.titech.ac.jp (S.I.), morimoto@eng.u-toyama.ac.jp (M.M.), fujimoto.keisuke@shizuoka.ac.jp (K.F.).

Abstract

Among the three primary colors, blue emission in organic light-emitting diodes (OLEDs) are highly important but very difficult to develop. OLEDs have already been commercialized; however, blue OLEDs have the problem of requiring a high applied voltage due to the high-energy of blue emission. Herein, an ultralow voltage turn-on at 1.47 V for blue emission with a peak wavelength at 462 nm (2.68 eV) is demonstrated in an OLED device. This OLED reaches 100 cd/m^2, which is equivalent to the luminance of a typical commercial display, at 1.97 V. Blue emission from the OLED is achieved by the selective excitation of the low-energy triplet states at a low applied voltage by using the charge transfer (CT) state as a precursor and the triplet-triplet annihilation, which forms one emissive singlet

from two triplet excitons. We found that the essential component for efficient blue emission is a smaller energy difference between the CT state and triplet exciton, accelerating the energy transfer between the two states and achieving the optimal performance by avoiding direct decay from the CT state to the ground state. Our study demonstrates that the developed OLED allows for a much longer operation lifetime than that from a typical blue phosphorescent OLED because the blue emission originates from a stable low-energy triplet exciton that avoids degrading the constituent materials.

Introduction

Blue is the most important constituent color in light-emitting devices because it has the highest energy among the three primary colors in displays, and white emission in lighting applications is made by a blue light source.[1] Organic light-emitting diodes (OLEDs) have already been commercialized in smartphones and large-screen displays, taking advantage of their ability to project high-color images with large contrast.[2] However, blue OLEDs still have drawbacks because of the need for a large applied voltage because the energy of blue emission can be as high as approximately 3 eV. Typical blue OLEDs need approximately 4 V for a luminance of 100 cd/m^2, which is a general display condition.[3] The industrial target is to operate blue OLEDs within 3.7 V, which is the rated voltage of the lithium-ion batteries that are loaded in most mobile devices. For this reason, blue OLEDs operating at low voltages are highly desirable for achieving commercial requirements.

Conventional fluorescent emitters are still used in commercial blue OLEDs due to their reliability and long operation lifetime,[4] although their external quantum efficiencies (EQE) in devices are lower than that of phosphorescent and thermally activated delayed fluorescence (TADF) materials; devices with phosphorescent and TADF materials are emerging technologies in academia.[5,6] The energy of the first triplet excited state (T_1) of anthracene derivatives, which are some of the most typical fluorescent emitters, is stable at 1.7 eV.[7] In contrast, blue phosphorescent and TADF materials have a T_1 that can be as high as 3 eV.[4] High energy levels are inevitable when considering their operating mechanism: the T_1 energies must be equal to or close to the blue light energy in the phosphorescent or TADF material. Here, the spin forbidden T_1 has a long lifetime, and 3 eV is equivalent to the dissociation

energy of a carbon-nitrogen bond.[8] Therefore, the high energy T_1 will promote the degradation of the material. This intrinsic problem prevents the commercialization of phosphorescent and TADF materials for blue OLEDs.[8]

The operation mechanism of a conventional fluorescent OLED is illustrated in **Figure 1a**. The formation ratios of the first singlet excited state (S_1) and T_1 are 25% and 75%, respectively, due to the spin statistic rule.[2] An applied voltage (V_{appl}) multiplied by the elementary charge (e) that is more than the bandgap energy of the emitter is needed to excite both the high-energy S_1 and low-energy T_1. This is because electrons and holes are independently injected from the charge transporting layers into the highest occupied molecular orbital (HOMO) and lowest unoccupied molecular orbital (LUMO) levels of the emitters, and the exciton binding energy and the extra energy related to the difference between S_1 and T_1 are lost to form T_1. A certain percentage of dark T_1 contributes to fluorescence through the triplet-triplet annihilation (TTA) process.[4] Therefore, we assumed that selective excitation of a low energy T_1 in a conventional emitter and subsequent TTA-based fluorescence with high efficiency enabled a dramatic reduction in the applied voltage.

The operational mechanism of the device called upconversion (UC)-OLED is illustrated in **Figure 1b**. Initially, holes and electrons are injected into donor (emitter) and acceptor (electron transport) layers, respectively, and recombine at the donor/acceptor (D/A) interface to form a charge transfer (CT) state. Subsequently, the energy of the CT state is transferred to T_1 of the emitter. Therein, blue light is emitted through the formation of high-energy S_1 by TTA. Due to the much lower energy of the CT state than the bandgap energy of the emitter, the UC process through TTA greatly reduces the applied voltage (V_{appl}) for exciting the emitter molecule compared to the conventional blue fluorescent OLED. The TTA-UC emission sensitized by the CT state has been mainly studied with rubrene, which shows yellow emission in previous studies.[9-13] From our experience, we obtained efficient blue TTA-UC emission by determining an appropriate combination of blue emitter (donor) and acceptor (electron transport) from 21 organic molecules. According to this design concept, the turn-on voltage of the blue OLED is greatly reduced to as low as 1.47 V, and the OLED reaches 100 cd/m^2, which is equivalent to the luminance of a typical display, at 1.97 V. Furthermore, the blue emission in the UC-OLED

originated from a stable low energy T_1 and subsequent fast TTA-UC emission,[14] which could potentially avoid degrading the constituent materials.

Results and Discussion

We utilized the anthracene derivative 1,2-ADN, which is one of the most widely used host materials in blue fluorescent OLEDs, as the emitter (donor) in our UC-OLEDs. Anthracene derivatives are also utilized as TTA emitters in the research field of photoexcited UC because they satisfy the energy requirements for efficient TTA: the energy of T_1 (1.7 eV) is slightly more than half the energy of S_1 (2.9 eV).[7,15,16] As a partner to form the D/A interface with 1,2-ADN, we investigated two phenyl pyridine derivatives (TmPyPB and B4PYMPM)[17,18] and a bipyridyl-substituted oxadiazole derivative (BPyOXD),[19] which are typical electron transport materials in conventional OLED devices, and a naphthalene diimide derivative with a fluorene side chain (NDI-HF).[20] NDI derivatives have strong electron acceptability; therefore, they are used as electron acceptors in the organic photovoltaic (OPV) field.[21] The energy levels of the materials are illustrated in **Figure 1c**. The HOMO levels of the electron transport materials are deeper than that of 1,2-ADN, whereas the LUMOs of electron transport (acceptor) materials lies in the order of TmPyPB, BPyOXD, B4PYMPM, and NDI-HF. We fabricated bilayer-type OLED devices with anthracene emitters and electron transport (acceptor) materials. The details of the device fabrication are described in the Supporting information.

The device properties of the OLED with 1,2-ADN and the four types of acceptor materials are exhibited in **Figure 2** and **S1**. Blue emission with a peak wavelength of 424 nm (2.92 eV) from 1,2-ADN is observed in all devices (**Figure 2a**); however, the luminance-voltage (*L-V*) characteristics in **Figure 2b** largely shift when different electron transport (acceptor) materials are used. The turn-on voltage, i.e., the voltage at which the electroluminescence (EL) emission reaches 1 cd/m^2,[12] is 4.3 V, 2.9 V, 3.0 V, and 1.7 V for TmPyPB, BPyOXD, B4PYMPM, and NDI-HF, respectively. Blue light can be emitted from approximately half the voltage of the photon energy in the 1,2-ADN/NDI-HF device.[9,10,12] This ultralow turn-on of blue emission is also observed when we use other anthracene derivatives and NDI-HF, as described in **Figure S2**.

To clarify the origin of the different turn-on voltages in these devices, we investigated the decay dynamics of EL emission (**Figure 2c)**. There is a clear difference in the transient EL signals between these devices using the different electron transport (acceptor) materials. The OLED devices with typical electron transport materials (TmPyPB, BPyOXD, and B4PYMPM) mainly show prompt decay, with EL lifetimes less than 0.1 μs (which is the detection limit of the instrument). The prompt decay is due to the fast emission from the S_1 states that form directly after charge injection to the emitter layer, as illustrated in **Figure 1a**.[22] The amplitude shows that approximately 90% of the EL emission is governed by fast emission in devices with the three typical electron transport materials. In contrast, only a slow decay component with a lifetime on the order of μs is observed in the EL decay curves of 1,2-ADN/NDI-HF. The slow decay can be associated with emission originating from the TTA of the triplet excitons, which is a slow diffusion process.[22] The results indicate that all of the emission in the 1,2-ADN/NDI-HF device is produced by TTA-UC and that the low energy T_1 of 1,2-ADN is selectively generated by charge injection (**Figure 1b**). The energy levels of S_1 and T_1 of 1,2-ADN are 2.9 and 1.7 eV, respectively.[7] The energy difference of the initial excited state produced by the injected charge results in the difference in turn-on voltage between the OLED with NDI-HF and other electron transport materials.

Note that the energy difference of LUMO between B4PYMPM and NDI-HF is only 0.1 eV; however, the turn-on voltage and the operation mechanism of the devices are clearly different. To elucidate the origin of the difference, we investigated the highly sensitive incident photon-to-current conversion efficiency (IPCE) to measure the CT state absorption, which reflected the D/A interaction at the interface between the emitter (donor) and the electron transport (acceptor) materials in **Figure 2d**.[23,24] The device with TmPyPB, BPyOXD, and B4PYMPM, which are typical electron transport materials in OLEDs, has little photocurrent response at wavelengths longer than the HOMO-LUMO transition of 1,2-ADN at approximately 450 nm. In contrast, the device with NDI-HF shows a clear photocurrent response until 700 nm, which is the signal of CT state formation at the D/A interface due to the strong interaction between 1,2-ADN and NDI-HF.[25] The results indicate that CT state formation is necessary

for the direct excitation of T_1 at low voltage because the CT state acts as a precursor for energy transfer to T_1, as illustrated in **Figure 1b**.

The next aspect is to determine if NDI-HF is the best acceptor material as the partner of 1,2-ADN for achieving efficient energy transfer from the CT state to T_1 of 1,2-ADN and consequently efficient TTA-UC emission. Therefore, we synthesized 14 NDI derivatives with a different substituent on the nitrogen position of NDI, as shown in **Figure 3a**. Details of the synthesis and the material properties are summarized in the Supporting Information. The substituents are broadly classified as aryl and alkyl groups. **Table S1** summarizes the LUMO energy levels of the NDI derivatives. Most NDIs with aryl groups have lower LUMO levels than NDIs with alkyl groups, as reflected by the difference in the electron donating properties from the substituents to the NDI core. The difference in the LUMO levels of NDI derivatives results in the large differences in the EL emission spectra of the UC-OLEDs. **Figure 3b** shows a typical example; the UC-OLED with NDI-HF containing an aryl group shows mostly TTA-UC emission at 450 nm, while the UC-OLED with NDI bearing a cyclohexyl group shows a clear CT emission at 665 nm (1.86 eV) appears with suppressed TTA-UC emission. The energy transfer scheme of the UC-OLED is illustrated in **Figure 3c**. TTA-UC emission occurs through energy transfer from the triplet CT state (CT_3) to T_1 of 1,2-ADN.[12] However, a direct decay path from the CT state to the ground state via either radiative or nonradiative transition also exists. To determine the relationship between the efficiency of TTA-UC emission and CT state energy, the TTA-UC emission intensity at constant current flow is plotted as a function of CT state energy in devices with the 14 NDI derivatives. The CT state energy is calculated by the peak wavelength of the CT emission in the EL spectra of the devices. We find a negative correlation; specifically, the TTA-UC emission intensity increases as the CT state energy decreases. Since the emission layers of all devices used the same 1,2-ADN, the difference in TTA-UC emission intensity was caused by the difference in energy transfer efficiency from CT_3 to T_1 of 1,2-ADN. The highest TTA-UC emission intensity was observed in the 1,2-ADN/NDI-HF device with a CT state energy of 1.71 eV (**Figure 3d**), which is very close to the peak energy of phosphorescence (1.77 eV) from T_1 of 1,2-ADN in solution at 77 K (**Figure S27**). Although the sample form and temperature of the measurement for the energy level are different, the

result clearly indicates that the proximity of the energy levels between the CT state and T_1 accelerates the energy transfer between the two excitonic states. The triplet energy transfer is governed by the Dexter mechanism.[26] Therefore, a larger spectral overlap between the two states will facilitate energy transfer.[27,28] Our finding is further supported by UC-OLEDs using another type of anthracene derivative TPA-An-mPhCz[29] with a 0.2 eV shallower HOMO level than 1,2-ADN and with a T_1 level almost identical to that of 1,2-ADN (**Figure S28**). Corresponding to the shallower HOMO level, the CT state energies of the device with TPA-An-mPhCz are 0.2–0.3 eV smaller than those of 1,2-ADN when the same NDI is used, as shown in **Figure S29**. Notably, the difference in the CT state energy changes the optimal acceptor partner for efficient TTA-UC emission in TPA-An-mPhCz. NDI-HF is the optimal for 1,2-ADN, whereas NDI-Cy with a shallower LUMO level relative to NDI-HF is optimal for TPA-An-mPhCz, as shown in the plot of the TTA-UC emission intensity of the devices (**Figure S29d**). The CT state energy of the TPA-An-mPhCz/NDI-HF device is as low as 1.40 eV; therefore, the energy transfer from the CT state to T_1 of the emitter is suppressed. With the optimal combination, the TPA-An-mPhCz/NDI-Cy device, which has close energy levels between the CT state and T_1 of the emitter, shows an ultralow turn-on voltage, similar to that observed for 1,2-ADN/NDI-HF (**Figure S30a**). Notably, B4PYMPM, which is a typical electron transport material with a deep LUMO level, does not function at a low turn-on voltage even with TPA-An-mPhCz, which has a shallower HOMO level. CT state absorption (**Figure S30b**) was observed in the TPA-An-mPhCz/NDI-Cy devices but not in the TPA-An-mPhCz/B4PYMPM device. This result further supports our conclusion that CT state formation at the D/A interface is essential for direct excitation of T_1 at an ultralow voltage.

Thus far, the best D/A combination, showing efficient TTA-UC emission, is 1,2-ADN/NDI-HF. We optimized the device structure by adding a typical blue fluorescent dopant, *tert*-butyl perylene (TbPe),[30] in the emitter layer. The device structure is illustrated in **Figure 4a**. The TbPe-doped layer is sandwiched by the undoped 1,2-ADN layer. The device concept is as follows: the core processes including CT state formation, energy transfer to T_1, and TTA occur near the D/A interface; however, the final emission occurs apart from the interface by Förster energy transfer to TbPe to suppress

interfacial quenching of the emissive S_1 exciton.[12] The EL emission spectrum and *L-V* curve of the optimized device are depicted in **Figure 4b, c**. The *J-V* curve and EL spectra at different current densities are shown in **Figure S31**. The device produced blue emission with a peak wavelength at 462 nm (2.68 eV) from TbPe. Notably, the turn-on voltage that shows 1 cd/m^2 was only 1.47 V, producing 100 cd/m^2 at 1.97 V. The high-energy blue emission is still observable at 1.26 V when sensitively measured by a photodiode. Blue emission of the UC-OLED is also visible by only connecting a 1.5 V battery, as shown in **Figure 4d**. Recently, several papers have been published reporting low-voltage operation of blue OLEDs.[31,32] However, the turn-on voltage was approximately 2.5 V. The ultralow voltage operation at approximately 1.5 V for blue emission has not been achieved even with inorganic LEDs.[33] Therefore, this is the lowest operating voltage thus far among any type of blue LED. The maximum EQE of the UC-OLED is 3.25% (**Figure 4e**), and the power efficiency is 3.04 lm/W (**Figure S32**); these are comparable to those of conventional blue fluorescent OLEDs.[3,34] The theoretical maximum EQE for the UC-OLED is calculated by multiplying the efficiency for every step used to produce blue emission; the spin statistics of triplet formation are 75%,[35] the maximum TTA efficiency is 50% because TTA is a two-photon process,[36] the measured photoluminescence QE of the TbPe-doped 1,2-ADN film is 73%, and the outcoupling efficiency is 20%.[37,38] Therefore, the theoretical maximum EQE for the blue UC-OLED is calculated to be 5.5%. There is still potential for the improvement of EQE by optimizing the device structure to achieve better performance. Note that the number of excitons is halved through TTA-UC. However, 37.5% corresponds to half of the formation ratio of T_1 (75%/2) and is still larger than 25%, which is the formation ratio of S_1 utilized in conventional fluorescent OLEDs.[2] Thus, both types of OLEDs can achieve comparable EQEs. The operation lifetime of the blue UC-OLED is compared to the device with a typical blue phosphorescent emitter, the bis-cyclometalated iridium (III) complex (FIrPic),[39,40] under the initial luminance condition at 1000 cd/m^2 (**Figure 4f**). The devices were simply encapsulated by UV resin and a cover glass without using desiccant and an oxygen scavenger. FIrPic exhibited phosphorescence from T_1 at a peak wavelength of 475 nm (2.61 eV), as shown in **Figure S33**. The lifetime for the luminance to decay to 50% from the initial luminance of 1000 cd/m^2 (LT_{50}) for the FIrPic device was found to be

approximately 3 h due to the device degradation by the high energy T_1. Conversely, the UC-OLED with a structure of **Figure 4a** provided an LT_{50} up to 270 h. This indicates that blue emission originating from low energy T_1 (1.77 eV in 1,2-ADN) is beneficial for device stability. Notably, the UC-OLED worked even without the LiF electron injection layer, as shown in **Figure S34**. This result was caused by a reduced energy barrier for electron injection due to the much lower LUMO level of NDI-HF than that of 1,2-ADN. An electron injection material such as LiF is one of the main causes of the reduced operational lifetime of OLEDs because of its air sensitivity.[41] Thus, the present UC-OLED system could have further enhanced the operation lifetime by avoiding the use of the problematic elements.

Finally, we discuss the origin of the extremely small starting voltage of the blue emission at 1.26 V, as shown in **Figure 4c**. To investigate the dependence of the applied electric field, the thickness dependence of the emission layer on the emissive properties was investigated. As shown in **Figure S35**, the threshold of the *L–V* curves was not shifted by the difference in the emission layer thickness between 25 and 100 nm. Specifically, the threshold voltage for the blue emission was not influenced by the electric field, indicating that the emissive properties were determined essentially by the D/A interface where the CT state formed. Note that 1.26 V, the threshold voltage for obtaining blue emission (**Figure 4c**), was much smaller than the CT state energy of 1,2-ADN/NDI-HF (1.71 eV) divided by the elementary charge. A recent report demonstrated that the EL emission in any type of inorganic and organic LED was observable by highly sensitive photon counting measurements at 0.5–1.0 V smaller than the bandgap energy of the emitter divided by the elementary charge.[33] The authors explained that the origin of the emission was the radiative recombination of nonthermal-equilibrium band-edge carriers whose populations were determined by the Fermi-Dirac function perturbed by a small external bias. In the case of organic semiconductors, band-edge carriers existed in the tail states inside the band gap of the material.[42] Those states determined the diode characteristic of the devices, especially near the threshold. The diode characteristic of our UC-OLED is shown in **Figure S36**. The threshold voltage of the diode for the current flow is at approximately 1.3 V, and the open-circuit

voltage (V_{OC}) of the UC-OLED under 1 sun irradiation is 1.32 V. These values correlate to an ultralow threshold voltage for blue light-emissive OLEDs.

Summary

In summary, we have demonstrated that the UC-OLED has ultralow turn-on voltage at 1.47 V for emitting blue light with a peak wavelength at 462 nm (2.68 eV) and reaches 100 cd/m^2, which is equivalent to the luminance of a typical display, at 1.97 V. Blue emission is achieved by the selective excitation of low-energy T_1 at low applied voltage and TTA-UC emission near the D/A interface. The essential factor is the appropriate choice of the D/A material to achieve the CT state formation and subsequent efficient energy transfer to T_1 of the emitter at the D/A interface. Our findings have a great impact on advancements in the field not only OLEDs but also OPVs because the T_1 formation at the D/A interface is currently considered the main cause of nonradiative recombination; this is the last challenging topic of OPVs for achieving a power conversion efficiency of over 20%.[43] We believe that the appropriate design of the D/A interface is essential for controlling the dynamics of excitonic processes,[44] leading to the development of efficient organic electronic devices and novel optoelectronic functions.

Author Contributions

S. I. conceived the idea, directed the project, fabricated the OLED devices, conducted the OLED characterization and wrote the majority of the paper. M. M. conducted the OLED characterization, especially the transient EL and luminance measurements using the photodiode. K. F. and K. B. designed and synthesized NDI derivatives. Y. M., M. T., S. N. and M. H. supervised the research. All the authors reviewed the manuscript.

Conflict of Interest

The authors declare no conflict of interest.

Acknowledgements

This research was supported in part by JSPS KAKENHI, Grants-in-Aid for Scientific Research (19K04465, 20KK0323, 21H05411, 22K14592), JST PRESTO (JPMJPR2101), a project (JPNP20004) subsidized by the New Energy and Industrial Technology Development Organization (NEDO), Izumi Science and Technology Foundation, Shorai Foundation for Science and Technology, and The Morino Foundation for Molecular Science. The authors would like to thank K. Tajima and K. Nakano at RIKEN for their assistance with the X-ray diffraction and photoelectron yield measurements.

References

1 Cho, J., Park, J. H., Kim, J. K. & Schubert, E. F. White light-emitting diodes: History, progress, and future. *Laser Photon. Rev.* **11**, 1600147 (2017).
2 Tsutsui, T. Progress in Electroluminescent Devices Using Molecular Thin Films. *MRS Bull.* **22**, 39-45 (2013).
3 Hu, J.-Y. *et al.* Bisanthracene-Based Donor-Acceptor-type Light-Emitting Dopants: Highly Efficient Deep-Blue Emission in Organic Light-Emitting Devices. *Adv. Funct. Mater.* **24**, 2064-2071 (2014).
4 Lee, J.-H. *et al.* Blue organic light-emitting diodes: current status, challenges, and future outlook. *J. Mater. Chem. C* **7**, 5874-5888 (2019).
5 Baldo, M. A. *et al.* Highly efficient phosphorescent emission from organic electroluminescent devices. *Nature* **395**, 151-154 (1998).
6 Uoyama, H., Goushi, K., Shizu, K., Nomura, H. & Adachi, C. Highly efficient organic light-emitting diodes from delayed fluorescence. *Nature* **492**, 234-238 (2012).
7 Lin, B. Y. *et al.* Exciplex-Sensitized Triplet-Triplet Annihilation in Heterojunction Organic Thin-Film. *ACS Appl. Mater. Interfaces* **9**, 10963-10970 (2017).
8 Wang, D., Cheng, C., Tsuboi, T. & Zhang, Q. Degradation Mechanisms in Blue Organic Light-Emitting Diodes. *CCS Chem.* **2**, 1278-1296 (2020).
9 Pandey, A. K. & Nunzi, J. M. Rubrene/Fullerene Heterostructures with a Half-Gap Electroluminescence Threshold and Large Photovoltage. *Adv. Mater.* **19**, 3613-3617 (2007).
10 Engmann, S. *et al.* Higher order effects in organic LEDs with sub-bandgap turn-on. *Nat. Commun.* **10**, 227 (2019).
11 Izawa, S. & Hiramoto, M. Efficient solid-state photon upconversion enabled by triplet formation at an organic semiconductor interface. *Nat. Photon.* **15**, 895-900 (2021).
12 Izawa, S., Morimoto, M., Naka, S. & Hiramoto, M. Efficient Interfacial Upconversion Enabling Bright Emission at an Extremely Low Driving Voltage in Organic Light‐Emitting Diodes. *Adv. Opt. Mater.* **10**, 2101710 (2022).
13 Yamada, M., Naka, S. & Okada, H. Light-emitting Organic Photovoltaic Devices Based on Rubrene/PTCDI-C13 Stack. *Electrochem.* **85**, 280-282 (2017).
14 Sakamoto, Y., Izawa, S., Ohkita, H., Hiramoto, M. & Tamai, Y. Triplet sensitization via charge recombination at organic heterojunction for efficient near-infrared to visible solid-state photon upconversion. *Commun. Mater.* **3**, 76 (2022).

15 Zhou, J., Liu, Q., Feng, W., Sun, Y. & Li, F. Upconversion luminescent materials: advances and applications. *Chem. Rev.* **115**, 395-465 (2015).
16 Yanai, N. & Kimizuka, N. New Triplet Sensitization Routes for Photon Upconversion: Thermally Activated Delayed Fluorescence Molecules, Inorganic Nanocrystals, and Singlet-to-Triplet Absorption. *Acc. Chem. Res.* **50**, 2487-2495 (2017).
17 Wu, S., Li, S., Sun, Q., Huang, C. & Fung, M. K. Highly Efficient White Organic Light-Emitting Diodes with Ultrathin Emissive Layers and a Spacer-Free Structure. *Sci. Rep.* **6**, 25821 (2016).
18 Sasabe, H. *et al.* Influence of Substituted Pyridine Rings on Physical Properties and Electron Mobilities of 2-Methylpyrimidine Skeleton-Based Electron Transporters. *Adv. Funct. Mater.* **21**, 336-342 (2011).
19 Ichikawa, M. *et al.* Bipyridyl oxadiazoles as efficient and durable electron-transporting and hole-blocking molecular materials. *J. Mater. Chem.* **16**, 221-225 (2006).
20 Tietze, M. L. *et al.* Passivation of Molecular n-Doping: Exploring the Limits of Air Stability. *Adv. Funct. Mater.* **26**, 3730-3737 (2016).
21 Zhang, G. *et al.* Nonfullerene Acceptor Molecules for Bulk Heterojunction Organic Solar Cells. *Chem. Rev.* **118**, 3447–3507 (2018).
22 Zhang, Y. & Forrest, S. R. Triplets contribute to both an increase and loss in fluorescent yield in organic light emitting diodes. *Phys. Rev. Lett.* **108**, 267404 (2012).
23 Vandewal, K., Tvingstedt, K., Gadisa, A., Inganas, O. & Manca, J. V. Relating the open-circuit voltage to interface molecular properties of donor:acceptor bulk heterojunction solar cells. *Phy. Rev. B* **81**, 125204 (2010).
24 Vandewal, K. *et al.* Increased open-circuit voltage of organic solar cells by reduced donor-acceptor interface area. *Adv. Mater.* **26**, 3839-3843 (2014).
25 Street, R. A. Electronic Structure and Properties of Organic Bulk-Heterojunction Interfaces. *Adv. Mater.* **28**, 3814-3830 (2016).
26 Dexter, D. L. A Theory of Sensitized Luminescence in Solids. *J. Chem. Phys.* **21**, 836-850, (1953).
27 Skourtis, S. S., Liu, C., Antoniou, P., Virshup, A. M. & Beratan, D. N. Dexter energy transfer pathways. *Proc. Natl. Acad. Sci. USA* **113**, 8115-8120 (2016).
28 Aizawa, N., Shikita, S. & Yasuda, T. Spin-Dependent Exciton Funneling to a Dendritic Fluorophore Mediated by a Thermally Activated Delayed Fluorescence Material as an Exciton-Harvesting Host. *Chem. Mater.* **29**, 7014-7022 (2017).
29 Han, P. *et al.* Aggregation-induced emission luminogen with excellent triplet-triplet upconversion efficiency for highly efficient non-doped blue organic light-emitting diodes. *Mater. Horiz.* **9**, 376-382 (2022).
30 Kim, S. K., Park, Y. I. & Park, J. W. Synthesis and Electroluminescent Properties of Fully Substituted Ethylene Moieties. *Mol. Cryst. Liq. Cryst.* **458**, 209-216 (2006).
31 Salehi, A. *et al.* Realization of high-efficiency fluorescent organic light-emitting diodes with low driving voltage. *Nat. Commun.* **10**, 2305 (2019).
32 Vasilopoulou, M. *et al.* High efficiency blue organic light-emitting diodes with below-bandgap electroluminescence. *Nat. Commun.* **12**, 4868 (2021).
33 Lian, Y. *et al.* Ultralow-voltage operation of light-emitting diodes. *Nat. Commun.* **13**, 3845 (2022).
34 Jiang, Y., Zhou, D.-Y., Dong, S.-C. & Tang, C. W. Impact of Chemical Degradation at HTL/EML Interface on Device Performance of Blue OLEDs. *SID Symposium Digest of Technical Papers* **50**, 252-255 (2019).
35 Sarma, M. & Wong, K. T. Exciplex: An Intermolecular Charge-Transfer Approach for TADF. *ACS. Appl. Mater. Interfaces* **10**, 19279-19304 (2018).
36 Di, D. *et al.* Efficient Triplet Exciton Fusion in Molecularly Doped Polymer Light-Emitting Diodes. *Adv. Mater.* **29**, 1605987 (2017).
37 Smith, L. H., Wasey, J. A. E. & Barnes, W. L. Light outcoupling efficiency of top-emitting organic light-emitting diodes. *Appl. Phys. Lett.* **84**, 2986-2988 (2004).

38 Furno, M., Meerheim, R., Hofmann, S., Lüssem, B. & Leo, K. Efficiency and rate of spontaneous emission in organic electroluminescent devices. *Phys. Rev. B* **85**, 115205 (2012).
39 Holmes, R. J. *et al.* Blue organic electrophosphorescence using exothermic host–guest energy transfer. *Appl. Phys. Lett.* **82**, 2422-2424 (2003).
40 Liu, Z., Helander, M. G., Wang, Z. & Lu, Z. Band Alignment at Anode/Organic Interfaces for Highly Efficient Simplified Blue-Emitting Organic Light-Emitting Diodes. *J. Phys. Chem. C* **114**, 16746-16749 (2010).
41 Fukagawa, H. *et al.* Highly efficient and air-stable inverted organic light-emitting diode composed of inert materials. *Appl. Phys. Express* **7**, 082104 (2014).
42 Yang, J.-P., Bussolotti, F., Kera, S. & Ueno, N. Origin and role of gap states in organic semiconductor studied by UPS: as the nature of organic molecular crystals. *J. Phys. D Appl. Phys.* **50**, 423002 (2017).
43 Gillett, A. J. *et al.* The role of charge recombination to triplet excitons in organic solar cells. *Nature* **597**, 666-671 (2021).
44 Imahori, H., Kobori, Y. & Kaji, H. Manipulation of Charge-Transfer States by Molecular Design: Perspective from "Dynamic Exciton". *Acc. Mater. Res.* **2**, 501-514 (2021).

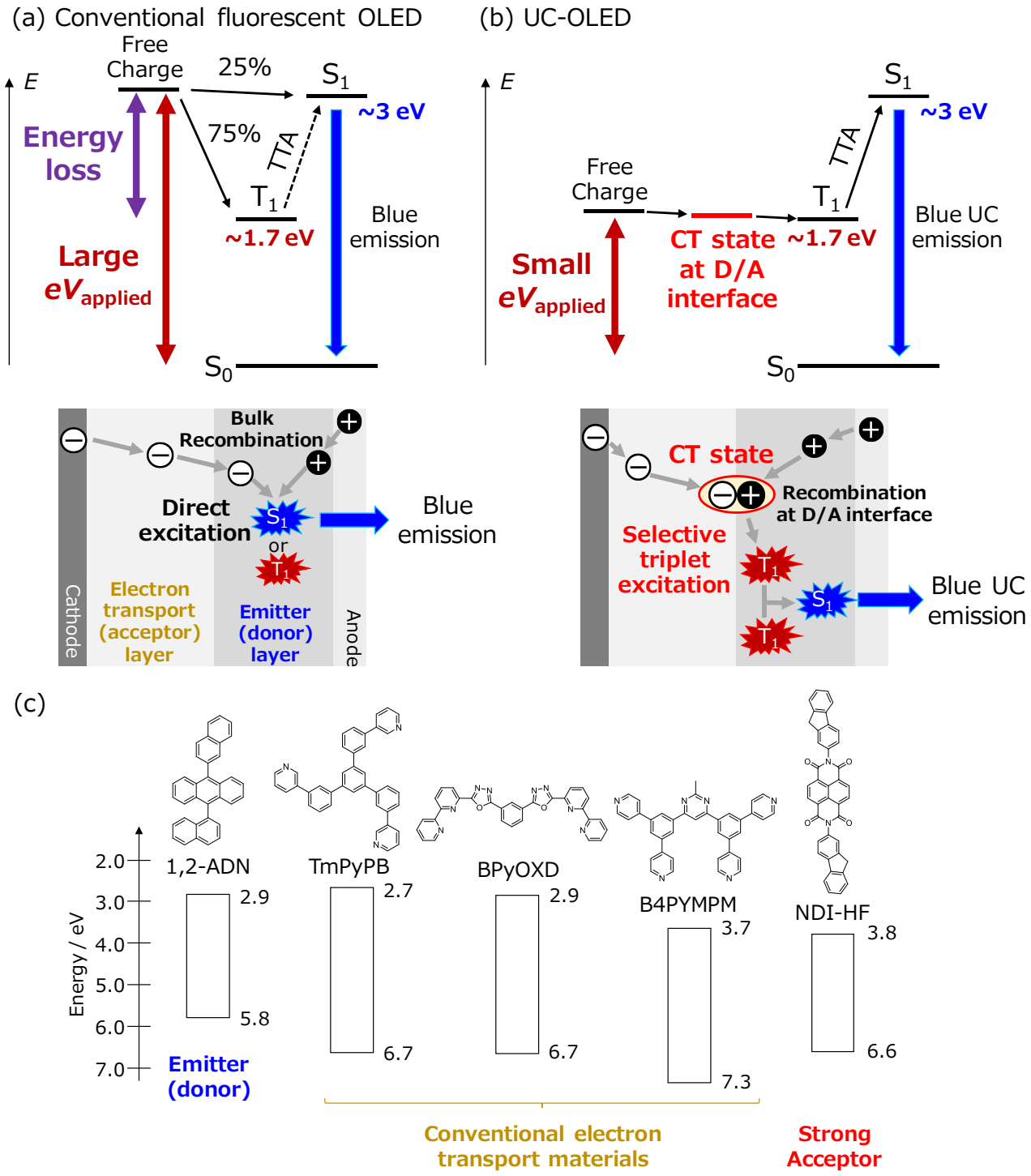

Figure 1. Schematic of the operating mechanism and the device structure of (a) a conventional blue fluorescent OLED and (b) a blue UC-OLED. (c) Chemical structures and energy levels of the materials.

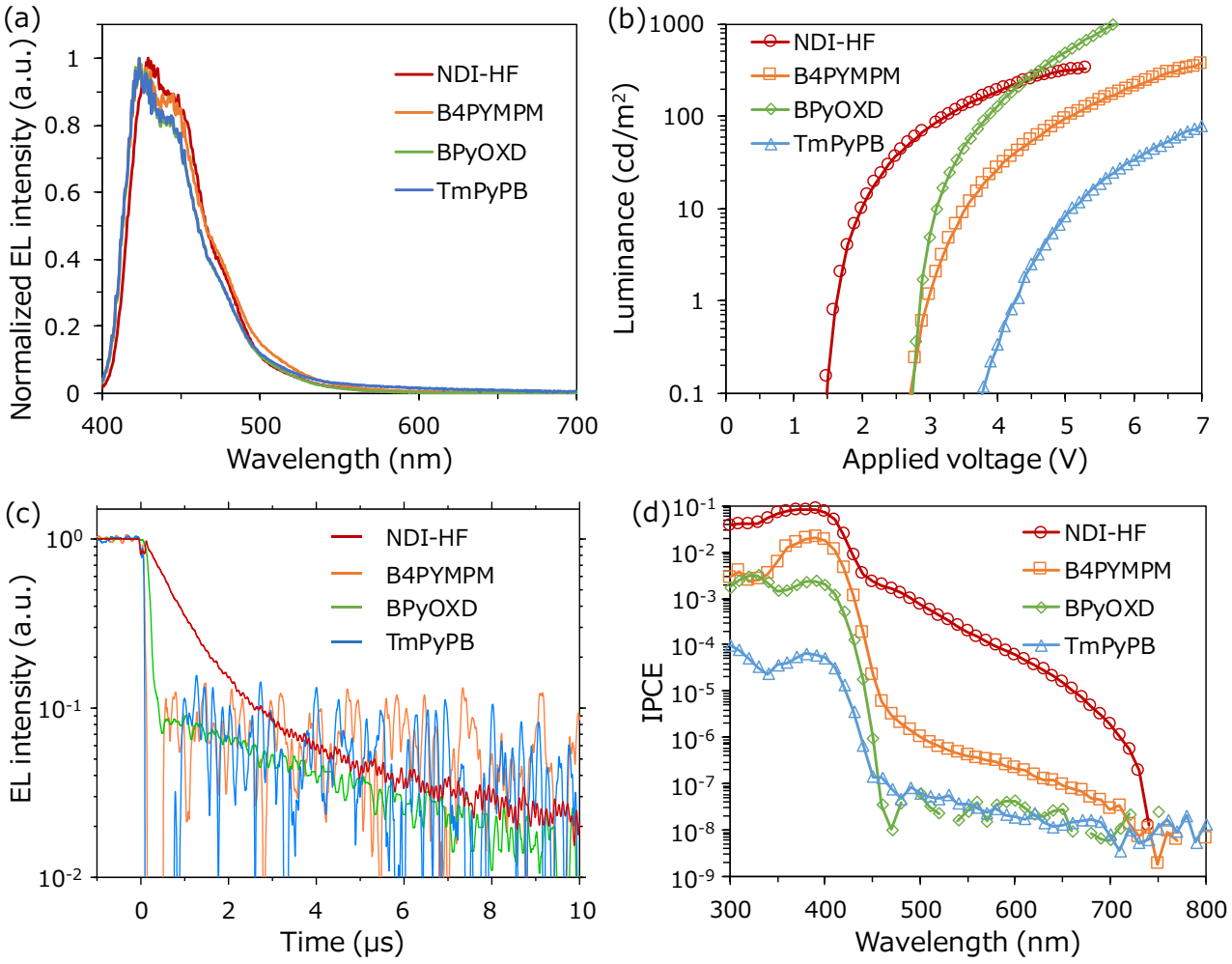

Figure 2. (a) EL emission spectra of the 1,2-ADN/NDI-HF (red), 1,2-ADN/B4PYMPM (orange), 1,2-ADN/BPyOXD (green) and 1,2-ADN/TmPyPB (blue) devices under a constant current flow (100 mA/cm^2). (b) *L*–*V* curves of the devices. (c) Decay dynamics of EL emission of the devices. Voltages of 3.5, 4.0, 4.0, and 6.0 V were applied to the 1,2-ADN/NDI-HF, 1,2-ADN/B4PYMPM, 1,2-ADN/BPyOXD and 1,2-ADN/TmPyPB devices, respectively. (d) Highly sensitive IPCE spectra of the devices.

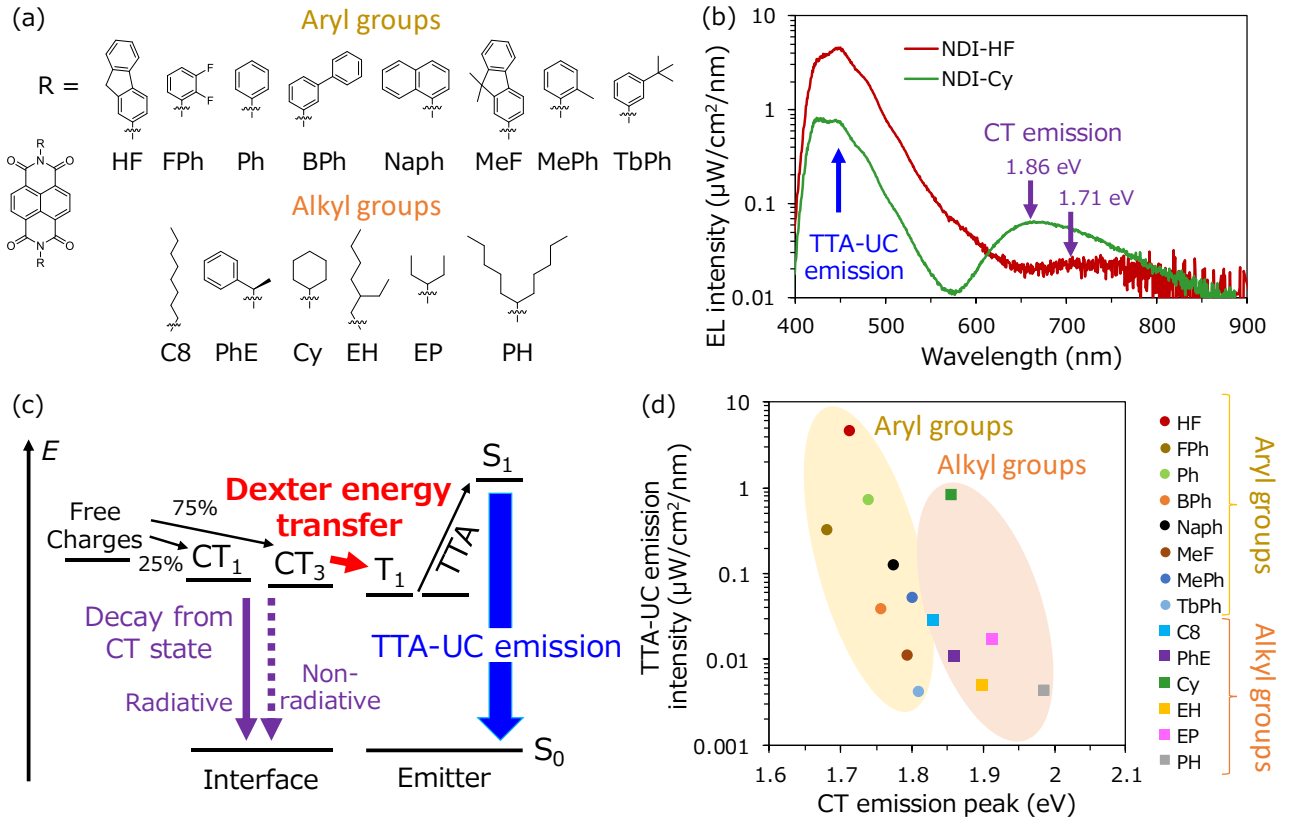

Figure 3. (a) Chemical structures of NDI derivatives. (b) EL emission spectra of the 1,2-ADN/NDI-HF (red) and 1,2-ADN/NDI-Cy (green) devices under a constant current flow (100 mA/cm^2). (c) Schematic of the energy transfer inside the UC-OLED. (d) Plots of the TTA-UC emission intensity versus energy of the CT emission peak for 1,2-ADN/NDI derivative devices.

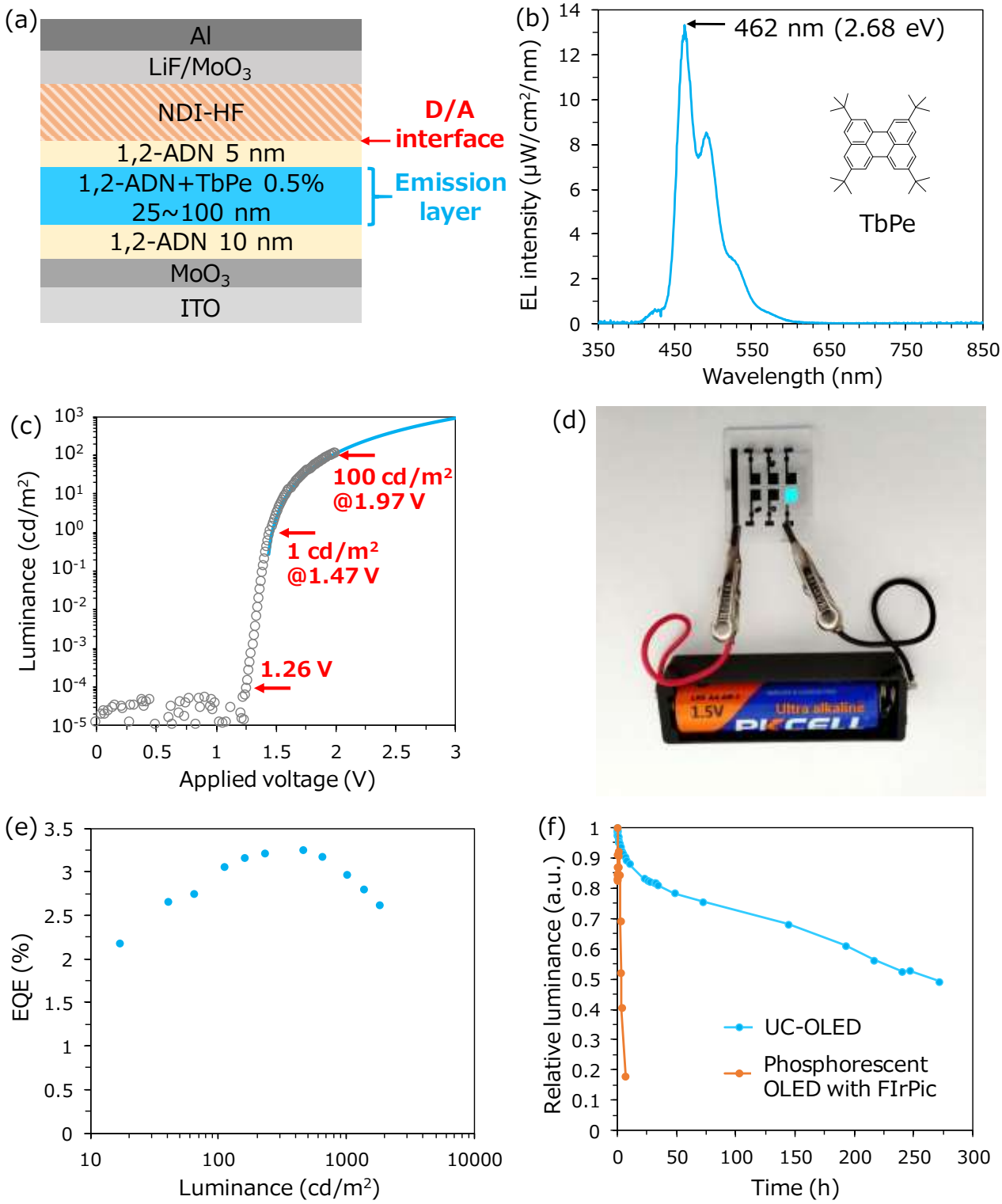

Figure 4. (a) Schematic of the optimized device structure with TbPe as a fluorescent dopant. (b) EL emission spectrum of the TbPe-doped 1,2-ADN/NDI-HF device under a constant current flow (100 mA/cm^2). The inset shows the chemical structure of TbPe. (c) *L*–*V* curves for the TbPe-doped device. The blue curve is measured by a luminance meter, and the gray circle is measured by the photodiode. The value of the photodiode is corrected by multiplying a coefficient to obtain the same value measured by the luminance meter. (d) Photograph of a TbPe-doped 1,2-ADN/NDI-HF device operated

by a 1.5 V battery. (e) EQE of the TbPe-doped 1,2-ADN/NDI-HF devices. (f) The operation lifetime measurement under the initial luminance condition at 1000 cd/m^2 of the TbPe-doped UC-OLED device (blue) and the FIrPic-doped phosphorescent device (orange).